

# Experimental Study on the Effect of Arm Design on the Performance of a Flap-Float Horizontal Ocean Wave Energy Converter

## Eksperimentalna studija o učinku dizajna poluge na izvedbu energije vala na horizontalnome ravnom plutajućem konverteru

Madi Madi\*

Institut Teknologi Sumatera  
Energy System Engineering  
South Lampung, Indonesia  
E-mail: madi@tse.itera.ac.id

Mukhtasor

Institut Teknologi Sepuluh Nopember  
Department of Ocean Engineering  
Surabaya, Indonesia  
E-mail: mukhtasor\_isp@yahoo.com

Rudi Walujo Prastianto

Institut Teknologi Sepuluh Nopember  
Department of Ocean Engineering  
Surabaya, Indonesia  
E-mail: rudiwp@gmail.com

Tuswan Tuswan

Universitas Diponegoro  
Department of Naval Architecture  
Semarang, Indonesia  
E-mail: tuswan@lecturer.undip.ac.id

Abdi Ismail

Indonesia Defense University  
Faculty of Vocational Studies  
Ship Machinery Study Program  
Belu, Indonesia  
E-mail: abdi.ismail@idu.ac.id

DOI 10.17818/NM/2022/2.1  
UDK 532.593  
627.223.6

Original scientific paper / Izvorni znanstveni rad  
Paper received / Rukopis primljen: 29. 12. 2021.  
Paper accepted / Rukopis prihvaćen: 29. 4. 2022.

### Abstract

Assessments on the configuration design of the ocean wave energy converter are fundamental to obtaining optimum performance under different environmental scenarios. In this study, the physical experimental test was conducted to investigate the suitable configuration of the proposed design of the Flap-Float Horizontal (FFH) energy converter device. A 1:20 scaled model was investigated in the laboratory tank subjected to normal wave conditions. Several parameters, including the arm length and angle of the buoy, were analyzed in different wave steepness to obtain the optimum arm design configuration. A total of 72 model tests were addressed to obtain a proposed maximum torque and voltage output. The result indicated that the best configuration design could be obtained by increasing the angle between the arm and the rope below the water level. In addition, it was discovered that the optimal configuration design with an angle of 88° and an arm length of 0.6 m yield the best results. The influence of the arm design sensitivity to various wave heights tended to be directly linear to the torque and voltage output. Finally, it was found that the greater the wave steepness, the bigger the output results.

### KEY WORDS

ocean wave energy  
flap-float horizontal  
arm design  
experimental test

### Sažetak

Procjena konfiguracije dizajna konvertera energije oceanskoga vala temeljna je za dobivanje najbolje izvedbe, prema različitim okolišnim scenarijima. U ovoj studiji izvodi se fizički eksperimentalni test da bi se ispitala prikladna konfiguracija predloženoga dizajna naprave FFH – horizontalnog ravnog plutajućeg konvertera. Model omjera A 1 : 2 ispituje se u laboratorijskome spremniku koji je izložen normalnim uvjetima vala. Različiti parametri, uključujući duljinu poluge i kut plutачe, analiziraju se u različitim strminama valova da bi se dobila najbolja konfiguracija dizajna poluge. Ispituju se ukupno 72 testna modela da bi se dobio najveći zakretni moment i output voltaže. Rezultat pokazuje da se najbolji dizajn konfiguracije može dobiti povećanjem kuta između poluge i konopa ispod površine vode. K tome, otkriveno da najpogodnija konfiguracija dizajna s kutom od 88 stupnjeva i duljinom poluge od 0,6 m donosi najbolje rezultate. Utjecaj osjetljivosti dizajna poluge na različite visine vala imao je tendenciju biti linearno povezan sa zakretnom silom i outputom voltaže. Najzad, ustanovljeno je da što je veća strmina, to su rezultati outputa veći.

### KLJUČNE RIJEČI

energija oceanskoga vala  
dizajn ravnoga plutajućega  
horizontalnoga konvertera  
eksperimentalni test

## 1. INTRODUCTION / Uvod

The Indonesian government, under presidential decree no. 5 of 2006, appointed a target aiming for a 17% contribution of renewable energy in the total primary energy integration

by 2025. In order to reach such objectives, research and assessments on renewable energy, specifically ocean renewable energy, have become a vital area in the recent decade. Indonesia, an archipelagic country with 65% of its territory being the sea,

\* Corresponding author

contains a tremendous amount of energy sources, including marine currents energy, ocean thermal energy, tidal energy, and wave energy. Investigations conducted by the Indonesian Agency for Assessment and Application of Technology revealed that west of Sumatera, south of Java, Bali, West Nusa Tenggara, and East Nusa Tenggara are very promising for wave energy generation [1].

Wave energy is generated into electricity through alternative energy movement effects of air pressure fluctuations caused by the wave motion [2]. Ocean wave energy has higher predictability and energy density content than wind and solar energy [3]. The first energy resource assessment in Indonesia over 6.5 years (2011-2017) showed that wave energy had been classified based on meteorological seasons. Besides, it was found that the most energetic months are June, July, and August for all areas of the south, southwest, and west of Indonesia [4]. In the south of Java island, Bali island, and West Nusa Tenggara, wave energy is available throughout the entire year. Based on those data, it is crucial to investigate wave energy design and performance research in Indonesia under different environmental scenarios.

Scholars have carried out a series of research on the design, characteristics, and mechanisms of numerous ocean wave energy. In general, ocean energy uses a generator to produce electrical energy, and the blade is the main component that can extract kinetic energy from mechanical motion [5,6]. Meanwhile, the potential application of other energy converters, including terminator, point absorber, and attenuator technology, are reviewed in detail in the references [7,8,9,10,11]. Further, the converter is usually equipped with a turbine, hydraulic, and generator power take-off (PTO) mechanism [8]. The existing ocean wave energy technology, namely, oscillating water column (OWC), pressure differential, floating structure, overtopping, and oscillating wave, are discussed in the references [7,8,9,11].

The recent global development of wave energy technology has resulted in a wide range of prototypes based on location grouping, working principles, and converters [12]. One of the novel wave energy converter types is Flap-Float Horizontal (FFH) energy converter device. The physical model of the FFH energy converter device is designed based on the onshore site using a single floating structure working principle and the absorber converter, which is inspired by the Wave Energy Converter (WEC) stationed at Hanstholm in the Danish Westcoast, see in literature [13]. The form of the WEC is called Wave Star Energy which consists of two or more point absorber converters [14,15,16,17]. In the example, the Wave Star Energy utilizing hydraulic power take-off mechanism has been developed both in numerical model simulations [18,19,20] and experimental models [21,22,23,24]. However, the application of the hydraulic PTO mechanism is not recommended due to high operation costs [25]. Besides, the previous study shows that the most critical part of the WEC and Wave Star Energy models is the arm as the main component of a hydrodynamic subsystem (HS) [25]. In this case, the length of the WEC and WaveStar's arms reported through experimental studies are 10 and 12 m [22,23]. Thus, the arm design is the most vital component to be analyzed as it links the point absorber and the PTO mechanism. Apart from the arm design, the work regarding the float design is essential to be noticed. The best float type in the WEC design is the hemisphere shape with a diameter of 5 m [22,23].

The above review of the ocean wave energy converter has been presented. However, limited studies were found to assess the configuration of the arm design of the ocean wave energy to obtain optimum performance in the Indonesian aquatic environment. In this regard, a laboratory-based test was conducted utilizing a scaled physical model of the FFH-type ocean wave energy converter under different environmental scenarios. The influence of the arm length, arm angle, and wave steepness parameters was investigated in a laboratory tank to obtain an optimum design configuration for the proposed FFH energy converter device. The water depth during the experiment was 0.65 m, which had been conditioned according to the conditions in the flume tank. The twelve wave steepness ( $H/gT^2$ ) used during the experiment have met the range of ( $H/gT^2$ )  $1 \times 10^{-4} - 119.6 \times 10^{-4}$ . This paper is organized as follows: Section 1 describes the research background and state of the art. Section 2 describes the theoretical background of the FFH energy converter device, and the experimental setup for laboratory tests is described in Section 3. Test results and discussions are presented in Section 4, followed by a conclusion and recommendation in Section 5.

## 2. THEORETICAL BACKGROUND / Teoretska pozadina

The buoy arm of the FFH energy converter device has a rotating axis at point A. The forces acting on the FFH energy converter device are analyzed at point B, as presented in Figure 1. Equation 1 explains a force equilibrium of the buoy for the motionless initial state.

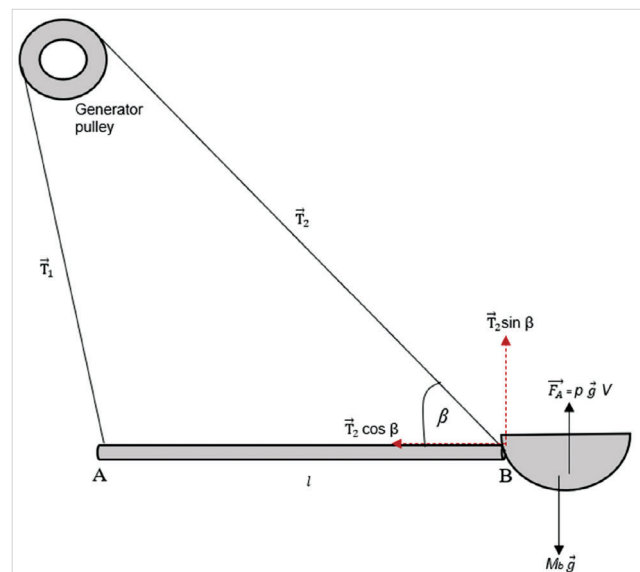


Figure 1 The forces acting on the FFH energy converter device  
Slika 1. Sile koje djeluju na FFH napravo – konverter energije

$$\sum \vec{F} = 0, \quad -M_b \vec{g} + \vec{F}_A + \vec{T}_2 \sin \beta = 0 \quad (1)$$

$$\vec{T}_2 \sin \beta = M_b \vec{g} - \vec{F}_A \quad (2)$$

$$\vec{T}_2 = \frac{M_b \vec{g} - \vec{F}_A}{\sin \beta} \quad (3)$$

In a motionless state, the pulley is also motionless thus,

$$\sum \tau = 0 \quad (4)$$

$$\vec{T}_1 R - \vec{T}_2 R = 0 \quad (5)$$

$$\vec{T}_1 = \vec{T}_2 = \frac{M_b \vec{g} - \vec{F}_A}{\sin \beta} \quad (6)$$

Where  $M_b$  is the mass of the buoy (kg),  $\vec{g}$  is the gravitational acceleration ( $m/s^2$ ),  $\vec{F}_A$  is the buoyant force (N),  $\vec{T}_1$  and  $\vec{T}_2$  are the belt tension,  $\beta$  is the buoy angle ( $^\circ$ ), and  $R$  is the radius (m). In the moving state, loosen up  $\vec{T}_2$  to 0, while  $\vec{T}_1$  is still in a tense state, so that:

$$\vec{\alpha} = \frac{(M_b \vec{g} - \vec{F}_A) R}{I_{generator} \sin \beta} \quad (7)$$

$$\frac{\vec{\omega}}{t} = \frac{(M_b \vec{g} - \vec{F}_A) R}{I_{generator} \sin \beta} \quad (8)$$

$$\vec{\omega} = \frac{(M_b \vec{g} - \vec{F}_A) R t}{I_{generator} \sin \beta} \quad (9)$$

$$\sum \tau = I \vec{\alpha} \quad (10)$$

$$\vec{T}_1 R - \vec{T}_2 R = I_{generator} \vec{\alpha} \quad (11)$$

$$\left( \frac{M_b \vec{g} - \vec{F}_A}{\sin \beta} \right) R - 0 = I_{generator} \vec{\alpha} \quad (12)$$

Where  $\vec{\omega}$  is the angular velocity (rad/s),  $\vec{\alpha}$  is the angular acceleration (rad/s<sup>2</sup>),  $t$  is time (s),  $I_{generator}$  is the moment inertia of the generator (kg.m<sup>2</sup>), and  $\tau$  is the torque (Nm).

### 3. DESCRIPTION OF MATERIALS AND EXPERIMENTAL SETUP / Opis materijala i eksperimentalne postavke

FFH energy converter device consists of 4 components: the reinforcing structure, generator, buoy arm, and buoy. The reinforcing structure and arms are made of steel. A half-spherical buoy made of styrofoam was chosen because this material floats more easily on the water surface. Then the styrofoam was coated with fiber and putty to make the buoy impermeable to water and stronger. After that, the finishing process was conducted by painting, leveling, and smoothing it with sandpaper, see Figure 2. During the experiments, the FFH converter system was excited in a flume tank (Figure 3) by the predetermined regular water wave field characterized by the wave height ( $H$ ) and period ( $T$ ), see Table 1. It aimed to determine the effect of the buoy angle ( $\beta$ ) and the wave condition or the wave steepness ( $H/gT^2$ ) on the torque (Nm) and the voltage (V). A 1:20 scaled model of the buoy was placed on the water surface ( $d$ ) with a depth of 0.65 m in the flume tank. The voltage was measured using a voltmeter connected directly to the generator pulley (Figure 3).



Figure 2 (a) The buoy was made of half-spherical styrofoam (b) The buoy was reinforced with a fiberglass layer  
Slika 2. (a) Plutača je napravljena od polusferične pur pjene (b) Plutača je ojačana premazom fiberglas

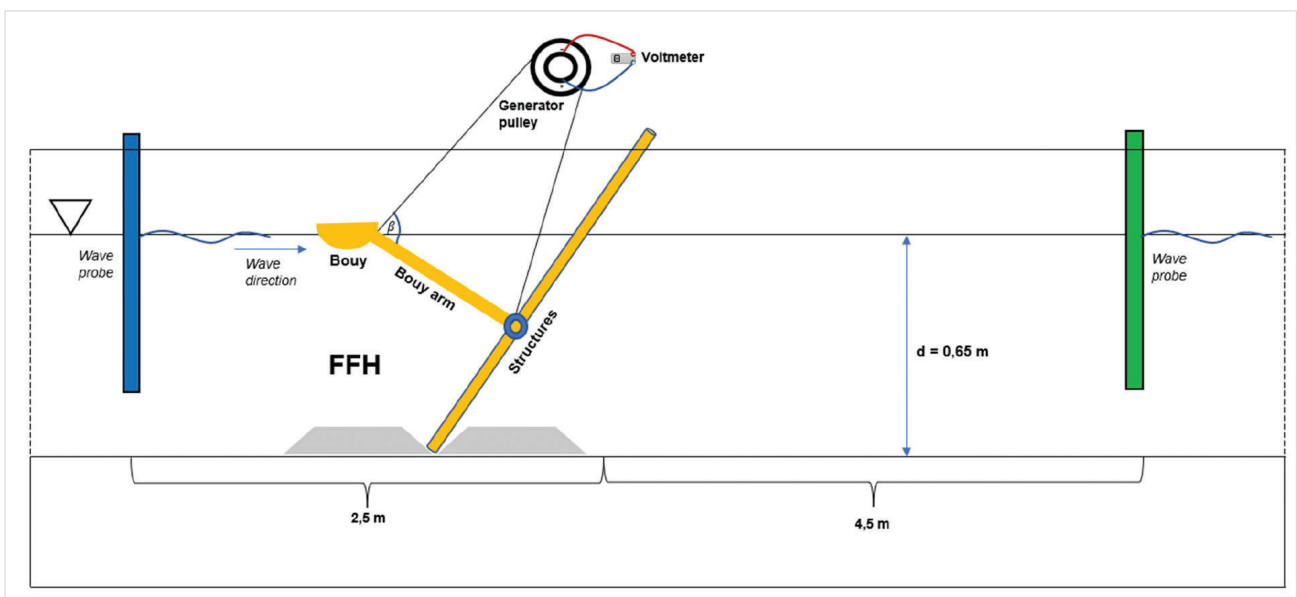


Figure 3 The FFH performance test scheme in a flume tank  
Slika 3. Testna shema izvedbe FFH u umjetnom vodenom spremniku

The height and period of the wave were adjusted to obtain a particular value of  $H/gT^2$  (wave parameter), as presented in Table 1. The environmental data were taken from the southern coast of Indonesia in Arafura, Natuna, and Situbondo, having an ocean wave steepness range ( $H/gT^2$ ) of  $1 \times 10^{-4} - 119.6 \times 10^{-4}$ . Table 2 below presents the length and the arm position to the water surface and the buoy angle ( $\beta$ ).

Table 1 Wave height and wave period for the FFH performance test  
Tablica 1. Visina i razdoblje vala za izvedbeni FFH test

No	H (m)	T (s)	$H/gT^2$ ( $10^{-4}$ )
1	0.0905	0.88	119
2	0.0855	0.90	107
3	0.0840	0.89	108
4	0.0770	0.89	99
5	0.0710	0.97	77
6	0.0680	0.82	103
7	0.0425	0.83	63
8	0.0145	0.59	43
9	0.0135	0.64	34
10	0.0065	0.65	16
11	0.0045	0.78	8
12	0.0010	0.88	1

Table 2 The arm length and position to the water surface and the buoy angle  
Tablica 2. Duljina poluge i položaj prema površini vode i kutu plutajuće

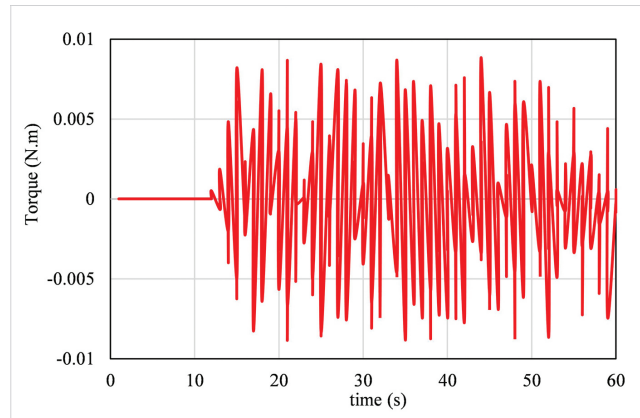
The length of the buoy arm (m)	The position of the buoy arm	$\beta$ (°)
0.4	Above the water surface	18
0.5	Above the water surface	19
0.6	Above the water surface	20
0.4	Below the water surface	67
0.5	Below the water surface	71
0.6	Below the water surface	88

## 4. RESULTS AND DISCUSSION / Rezultati i rasprava

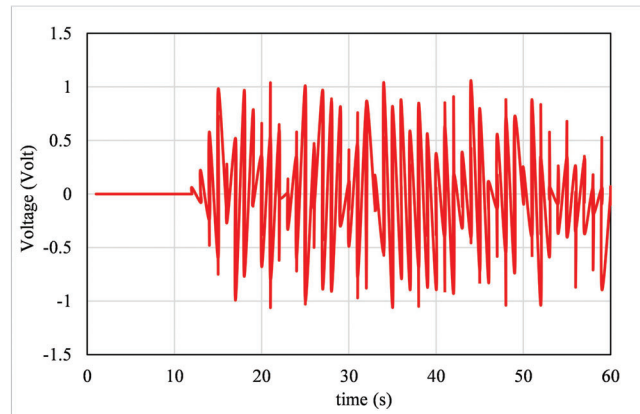
### 4.1. Conditions of physical experimental test / Uvjeti fizičkoga eksperimentalnog testa

An experimental test on Flap-Float Horizontal (FFH) - type ocean wave energy converter under normal wave conditions to investigate the effect of proposed parameters is reviewed in this section. The input parameters, including wave steepness ( $H/gT^2$ ) and angle variations ( $\beta$ ), were designed with 12 variations of wave steepness, and six variations of angle were tested for 60 s to obtain data on the torque and voltage output. The six angle variations ( $\beta$ ) corresponding to the arm length above and below water levels were  $18^\circ$ ,  $19^\circ$ ,  $20^\circ$ ,  $67^\circ$ ,  $71^\circ$ , and  $88^\circ$ . A total of 72 tests were conducted to observe the relationship between those wave steepness under different angle variations and calculate the maximum torque and voltage output. An example of the test results to depict the relationship between the time series and the torque and voltage output is illustrated in Figure 4. For instance, the relationship between the torque output and the time series of the model using a wave steepness of  $H = 0.0905$  m and  $T = 0.88$  s, and an angle ( $\beta$ ) of  $18^\circ$  is illustrated in Figure 4a. From these results, the maximum measured torque output was obtained at 44 s with a magnitude of  $88 \times 10^{-4}$  Nm, and the average torque output was obtained with a magnitude of  $18.4 \times 10^{-4}$  Nm. Moreover, Figure 4b presents the relationship

between the voltage output and the time series of the model using a wave steepness of  $H = 0.0905$  m and  $T = 0.88$  s and an angle ( $\beta$ ) of  $18^\circ$ . The maximum voltage output was obtained at 44 s with a magnitude of 1.06 volts, and the average voltage output was obtained with a magnitude of 0.221 volts.



(a)



(b)

Figure 4 Output time response of the model with an angle of  $180$  and a wave steepness of ( $H/gT^2$ )  $119 \times 10^{-4}$ , where  $a =$  torque and  $b =$  voltage

Slika 4. Output vremenskog odgovora modela s kutom od  $18$  stupnjeva i strminom vala od ( $H/gT^2$ )  $119 \times 10^{-4}$ , gdje je  $a =$  zakretna sila,  $b =$  voltaža

### 4.2. Relationship between the angle variations and the torque and voltage output / Odnos između varijacija kuta te outputa zakrivljenosti i voltaže

In this section, the relationship between the variation of the buoy angles ( $\beta$ ) above the water ( $18^\circ$ ,  $19^\circ$ ,  $20^\circ$ ) and below the water ( $67^\circ$ ,  $71^\circ$ ,  $88^\circ$ ) as stated in Table 2 and the variation of the wave steepness ( $H/gT^2$ )  $1 \times 10^{-4} - 119 \times 10^{-4}$  as stated in Table 1 on the torque and voltage output is reviewed. This study aims to obtain the best arm design configuration with the highest torque and voltage output. The relationship between the arm angle variations of  $18^\circ$ ,  $19^\circ$ , and  $20^\circ$  with the position above the water level and at various wave steepness is figured out in Figure 5a. It was found that the higher the angle of the arm and the rope, the bigger the torque output for all wave steepness. It was also found that an arm design with a length of 0.4 m and an angle of  $18^\circ$  above the water level had the smallest torque output. In contrast, the highest torque output was obtained in the arm design with a length of 0.6 m and an angle of  $20^\circ$  above

the water level. Similar arm lengths using different angles with a position below the water level were compared to perform a more comprehensive analysis. Figure 5b compares the torque output at the angle variations positioned below the water level analyzed in 12 variations of wave steepness ( $H/gT^2$ ) as stated in Table 1. Similarly, the results indicated that increasing the angle caused an increase in the torque output in all wave steepness ( $H/gT^2$ ). In conclusion, the lowest torque output of the model was obtained with an arm length and angle of 0.4 m and  $67^\circ$ , respectively. On the other hand, the highest torque of the model was obtained with an arm length of 0.6 m and an angle of  $88^\circ$ . Besides the torque output, an analysis of the influence of the arm design variations on the voltage output is necessary. The relationship between the arm angle and position above the water level and the voltage output at different wave steepness ( $H/gT^2$ ), as stated in Table 1, is presented in Figure 6a. Similar to the previous torque output results, it can be observed that the bigger the angle of the arm design, the higher the voltage output for all wave steepness ( $H/gT^2$ ). Besides, the lowest voltage output was found in the model with an angle of  $18^\circ$ , while the highest voltage output of the model was obtained with an angle of  $20^\circ$  above sea level. Moreover, the voltage output of the model using angle variations below sea level is illustrated in Figure 6b. It was found that the highest voltage output was obtained with an arm angle of  $88^\circ$ , and the lowest voltage output was obtained with an arm angle of  $67^\circ$  below sea level.

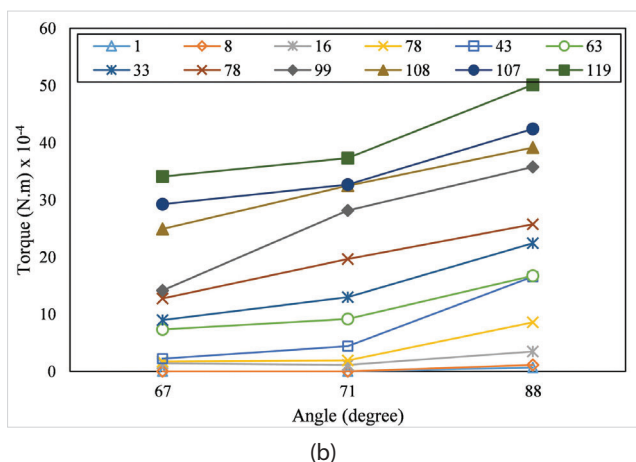
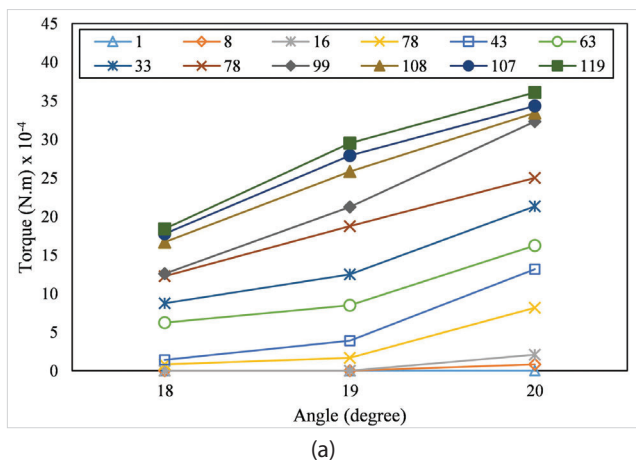


Figure 5 Relationship between the arm torque and angle variations at different wave steepness, where a = above water level and b = below water level

Slika 5. Odnos između zakretne sile poluge i varijacija kuta pri različitim strminama vala, gdje je a = iznad razine vode, a b = ispod razine vode

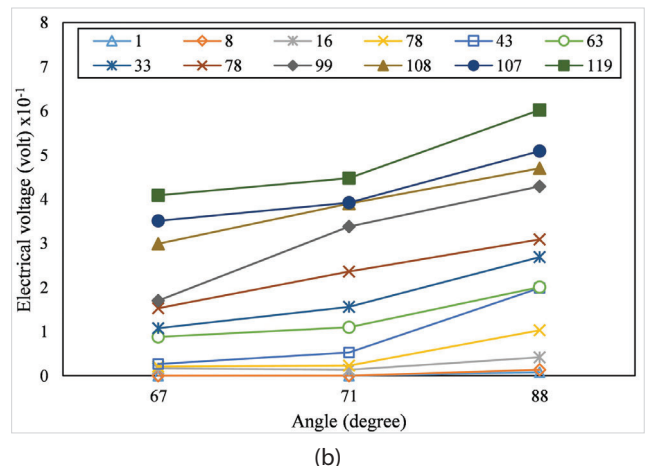
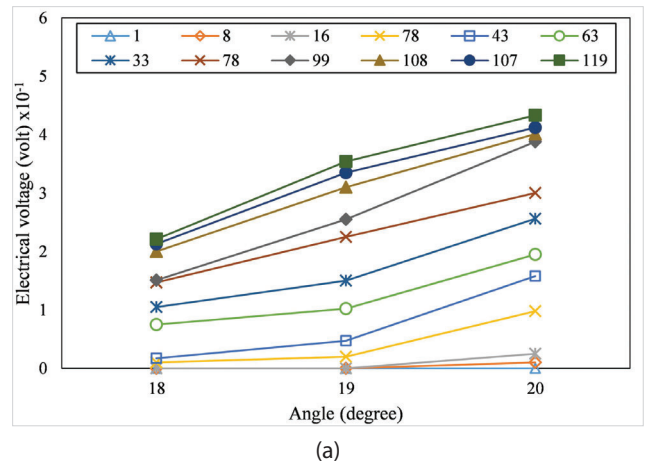
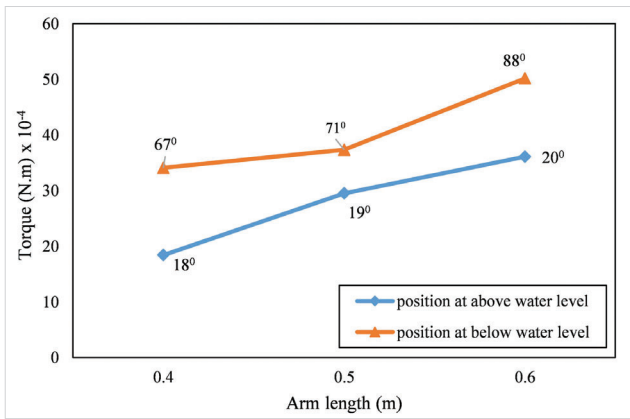


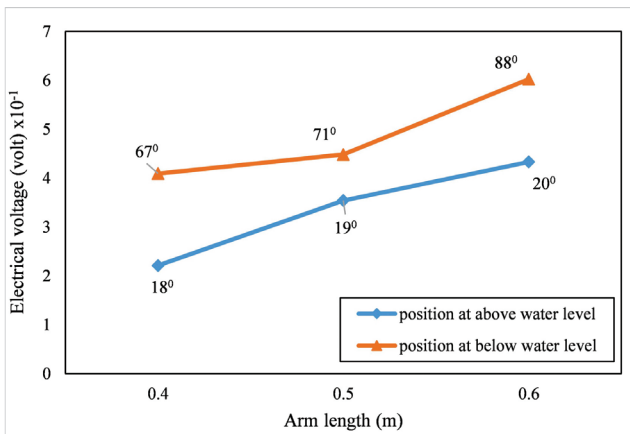
Figure 6 Relationship between the arm voltage and angle variations at different wave steepness, where a = above water level and b = below water level

Slika 6. Odnos između voltaže poluge i varijacija kuta na različitim strminama vala, gdje je a = iznad razine vode, a b = ispod razine vode

Furthermore, it is important to compare the torque and voltage output between the angle variations below and above the water level. Figure 7 illustrates the comparison between the arm position and the torque and voltage output at a wave steepness ( $H/gT^2$ ) of  $119 \times 10^{-4}$ . A similar phenomenon was found between the torque and voltage output. It was found that the arm design with an equivalent length and an angle below the water level was more effective and generated a higher output than the arm design with the same angle above the water level. In addition, it was found that the arm design with an angle of  $88^\circ$  and a length of 0.6 m was the best design configuration. The analysis results also indicated that the arm models with higher angles generated higher angular velocity. The arm model with higher angular velocity can move with a higher deviation. With a higher angle, the buoy is also easier to move with the amplitude of the wave motion.



(a)



(b)

Figure 7 Comparison between the arm position and the output value at a wave steepness of  $119 \times 10^{-4}$ , where a = torque and b = voltage

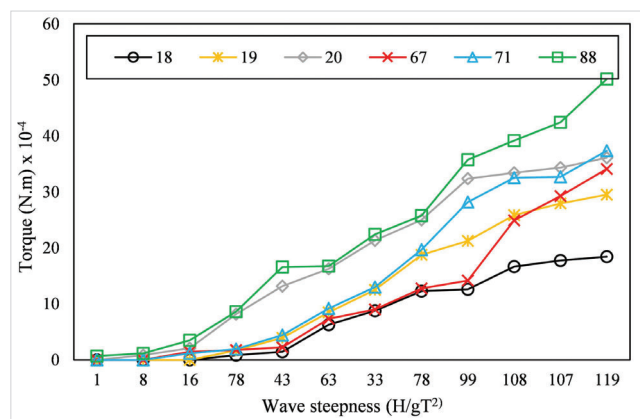
Slika 7. Usporedba između položaja poluge i vrijednosti outputa pri strmini vala od  $119 \times 10^{-4}$ , gdje je a = zakretna sila, a b = voltaža

#### 4.3. Analysis of design sensitivity to environmental conditions / Analiza osjetljivosti dizajna na okolišne uvjete

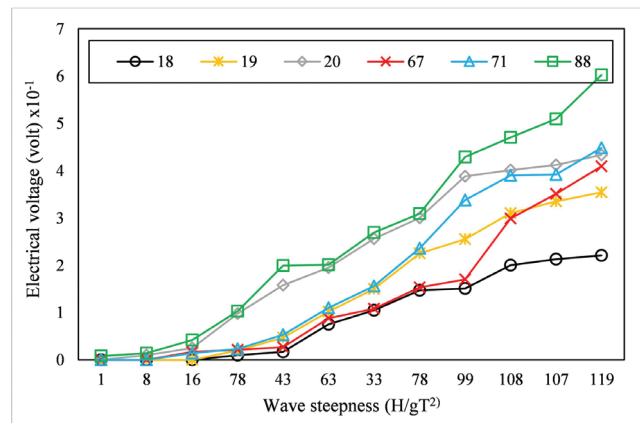
This section discusses the sensitivity of the arm design with various angles to various environmental conditions, such as wave steepness variations. The influence of the torque output with various angles and under different wave steepness ( $H/gT^2$ ), as stated in Table 1, is presented in Figure 8a. The analysis results explained that wave steepness ( $H/gT^2$ ) affected the torque output. In addition, the highest torque output was obtained in the design model with an angle of  $88^\circ$  at a wave height of 9.05 m with  $T = 0.88$  s. Moreover, Figure 8b illustrates the influence of voltage output with the arm angle variations under different wave steepness ( $H/gT^2$ ), as stated in Table 1. It was found that the higher the wave steepness ( $H/gT^2$ ), the higher the voltage output generated by the model. The highest voltage was recorded in the design model with an angle of  $88^\circ$  at a wave height of 9.05 m with  $T = 0.88$  s. Based on the results presented in Figure 8, the higher the wave, the greater the output generated by the model.

### 5. CONCLUSION / Zaključak

The experimental laboratory test was conducted to develop a 1:20 scaled model of an FFH-type ocean wave energy converter. The effect of the arm design of the FFH energy converter device on the torque and voltage output has been comprehensively reviewed in the previous sections with the following conclusions:



(a)



(b)

Figure 8 Comparison between the output value and the wave steepness at the arm angle variations, where a = torque and b = voltage

Slika 8. Usporedba između vrijednosti outputa i strmine vala na varijacijama kuta poluge, gdje je a = zakretna sila, a b = voltaža

1. The increase in the angle between the arm and the rope of the buoy, whether the arm is below or above the water level, causes an increase in the torque and voltage output. It was found that the best configuration design with an arm angle of  $88^\circ$  and an arm length of 0.6 m generates the maximum result. The optimum FFH conversion energy device design is when the arm of the buoy is positioned below the free surface.
2. The influence of the arm design sensitivity to various environmental conditions tends to be directly proportional to the torque and voltage output. In addition, the height of the wave ( $H$ ) is directly proportional to the torque and voltage output. The bigger the wave steepness ( $H/gT^2$ ), the greater the output results. Finally, the highest output result was obtained at the wave steepness ( $H/gT^2$ ) of  $119 \times 10^{-4}$ , at the wave height ( $H$ ) of 0.905 m, and at the period ( $T$ ) of 0.88 s. Based on the results of this study, further studies are suggested to address and investigate the performance of the arm design of the FFH ocean wave energy converter using irregular waves.

### ACKNOWLEDGEMENT / Zahvala

The authors offer their greatest gratitude to the Laboratory of Environment and Marine Energy of Institut Teknologi Sepuluh Nopember for supporting and facilitating this experimental test.

## REFERENCES / Literatura

- [1] Ribal, A.; Zieger, S. (2016). "Wave energy resource assessment based on satellite observations around Indonesia". AIP Conference Proceedings, Vol. 1737, No. 1, p. 060001. <https://doi.org/10.1063/1.4949308>
- [2] Djatmiko, E. B. (2012). *Perilaku dan Operabilitas Bangunan Laut di Atas Gelombang Acak*. Surabaya, Indonesia: ITS-Press.
- [3] Chozas, J. F. (2013). *Technical and non-technical issues towards the commercialization of wave energy converters*. Denmark: River Publishers. <https://doi.org/10.13052/rp-9788793102538>
- [4] Ribal, A.; Babanin, A. V.; Zieger, S.; Liu, Q. (2020). "A high-resolution wave energy resource assessment of Indonesia". *Renewable Energy*, Vol. 160, pp. 1349-1363. <https://doi.org/10.1016/j.renene.2020.06.017>
- [5] Madi, Sasono, M. E. N.; Hadiwidodo, Y. S.; Sujiatanti, S. H. (2019). "Application of savonius turbine behind the propeller as energy source of fishing vessel in indonesia". *IOP Conference Series: Materials Science and Engineering*, Vol. 588, No. 1. <https://doi.org/10.1088/1757-899X/588/1/012046>
- [6] Madi, M.; Tuswan, T.; Arirohman, I. D.; Ismail, A. (2021). "Comparative Analysis of Taper and Taperless Blade Design for Ocean Wind Turbines in Ciheras Coastline, West Java". *Kapal: Jurnal Ilmu Pengetahuan dan Teknologi Kelautan*, Vol. 18, No. 1, pp. 8-17. <https://doi.org/10.14710/kapal.v18i1.32486>
- [7] Drew, B.; Plummer, A. R.; Sahinkaya, M. N. (2009). "A review of wave energy converter technology". *Proceedings of the Institution of Mechanical Engineers, Part A: Journal of Power and Energy*, Vol. 223, No. 8, pp. 887-902. <https://doi.org/10.1243/09576509JPE782>
- [8] Antonio, F. D. O. (2010). "Wave energy utilization: A review of the technologies". *Renewable and sustainable energy reviews*, Vol. 14, No. 3, pp. 899-918. <https://doi.org/10.1016/j.rser.2009.11.003>
- [9] Lagoun, M. S.; Benalia, A.; Benbouzid, M. H. (2010). "Ocean wave converters: State of the art and current status". *IEEE International Energy Conference*, pp. 636-641. <https://doi.org/10.1109/ENERGYCON.2010.5771758>
- [10] Czech, B.; Bauer, P. (2012). "Wave energy converter concepts: Design challenges and classification". *IEEE Industrial Electronics Magazine*, Vol. 6, No. 2, pp. 4-16. <https://doi.org/10.1109/MIE.2012.2193290>
- [11] López, I.; Andreu, J.; Ceballos, S.; De Alegría, I. M.; Kortabarria, I. (2013). "Review of wave energy technologies and the necessary power-equipment". *Renewable and sustainable energy reviews*, Vol. 27, pp. 413-434. <https://doi.org/10.1016/j.rser.2013.07.009>
- [12] Pelc, R.; Fujita, R. M. (2002). "Renewable energy from the ocean". *Marine Policy*, Vol. 26, No. 6, pp. 471-479. [https://doi.org/10.1016/S0308-597X\(02\)00045-3](https://doi.org/10.1016/S0308-597X(02)00045-3)
- [13] Zurkinden, A. S.; Lambertsen, S. H.; Damkilde, L. (2012). "Structural Modeling and Analysis of a Wave Energy Converter". *Proceedings of the 25th Nordic Seminar on Computational Mechanics*. Lund University. <https://doi.org/10.1115/OMAE2013-10854>
- [14] Kofoed, Peter J.; Frigaard, P.; Kramer, M. (2016). "Recent developments of wave energy utilization in Denmark". *Proceedings of the Workshop on Renewable Ocean Energy Utilization: the 20th annual conference*. Korean Society of Ocean Engineers.
- [15] Hansen, R. H.; Kramer, M. M. (2011). "Modelling and control of the wavestar prototype". *Proceedings of the 9th European Wave and Tidal Energy Conference, EWTEC*. University of Southampton.
- [16] Babarit, A.; Hals, J.; Muliawan, M. J.; Kurniawan, A.; Moan, T.; Krokstad, J. (2012). "Numerical benchmarking study of a selection of wave energy converters". *Renewable energy*, Vol. 41, pp. 44-63. <https://doi.org/10.1016/j.renene.2011.10.002>
- [17] Zurkinden, A. S.; Jepsen, M. S.; Sichani, M. T.; Damkilde, L. (2014). "Nonlinear Motion Analysis of the Wavestar Wave Energy Converter With a Focus on the Structural Responses". *International Conference on Offshore Mechanics and Arctic Engineering*, Vol. 45530, p. V09AT09A045. American Society of Mechanical Engineers. <https://doi.org/10.1115/OMAE2014-23796>
- [18] Costello, R.; Ringwood, J.; Weber, J. (2011). "Comparison of two alternative hydraulic PTO concepts for wave energy conversion". *Proceedings of the 9th European wave and tidal energy conference (EWTEC)*. School of Civil Engineering and the Environment, University of Southampton.
- [19] Zhang, D.; Li, W.; Lin, Y.; Bao, J. (2012). "An overview of hydraulic systems in wave energy application in China". *Renewable and Sustainable Energy Reviews*, Vol. 16, No. 7, pp. 4522-4526. <https://doi.org/10.1016/j.rser.2012.04.005>
- [20] Hansen, R. H.; Kramer, M. M.; Vidal, E. (2013). "Discrete displacement hydraulic power take-off system for the wavestar wave energy converter". *Energies*, Vol. 6, No. 8, pp. 4001-4044. <https://doi.org/10.3390/en6084001>
- [21] Henderson, R. (2006). "Design, simulation, and testing of a novel hydraulic power take-off system for the Pelamis wave energy converter". *Renewable energy*, Vol. 31, No. 2, pp. 271-283. <https://doi.org/10.1016/j.renene.2005.08.021>
- [22] Marquis, L.; Kramer, M.; Frigaard, P. (2010, October). "First power production figures from the wave star roshage wave energy converter". *Proceedings of the 3rd International Conference on Ocean Energy (ICOE-2010)*. Bilbao, Spain, Vol. 68, pp. 1-5.
- [23] Kramer, M.; Marquis, L.; Frigaard, P. (2011). "Performance evaluation of the wavestar prototype". *9th ewtec 2011: Proceedings of the 9th European Wave and Tidal Conference*, Southampton, UK, 5th-9th September 2011. University of Southampton.
- [24] Lasa, J.; Antolin, J. C.; Angulo, C.; Estensoro, P.; Santos, M.; Ricci, P. (2012). "Design, construction and testing of a hydraulic power take-off for wave energy converters". *Energies*, Vol. 5, No. 6, pp. 2030-2052. <https://doi.org/10.3390/en5062030>
- [25] Ferri, F. (2014). *Wave-to-wire modelling of wave energy converters: Critical assessment, developments and applicability for economical optimization*.